Magnetic Resonance in Medicine 42:515–525 (1999)

Optimal Strategies for Measuring Diffusion in Anisotropic Systems by Magnetic Resonance Imaging

D.K. Jones,[1] M.A. Horsfield,[1]* and A. Simmons[2,3]

The optimization of acquisition parameters for precise measurement of diffusion in anisotropic systems is described. First, an algorithm is presented that minimizes the bias inherent in making measurements with a fixed set of gradient vector directions by spreading out measurements in 3-dimensional gradient vector space. Next, it is shown how the set of *b*—matrices and echo time can be optimized for estimating the diffusion tensor and its scalar invariants. The standard deviation in the estimate of the tensor trace in a water phantom was reduced by more than 40% and the artefactual anisotropy was reduced by more than 60% when using the optimized scheme compared with a more conventional scheme for the same scan time, and marked improvements are demonstrated in the human brain with the optimized sequences. Use of these optimal schemes results in reduced scan times, increased precision, or improved resolution in diffusion tensor images. Magn Reson Med 42:515–525, 1999. © **1999 Wiley-Liss, Inc.**

Key words: diffusion tensor; anisotropy; magnetic resonance; optimization

Precise assessment of diffusion by magnetic resonance spectroscopy or imaging requires a high signal-to-noise ratio for the unweighted and diffusion-weighted measurements, or requires that many measurements of signal attenuation are made. Optimal data collection schemes have been devised for isotropic media, or for estimates of diffusivity along one direction (1–7). However, with one exception involving optimization of an isotropically weighted scheme for estimation of the diffusion tensor trace (8), the problem of maximizing the precision of measurement of diffusion in anisotropic systems has not been tackled. Poor estimation of the diffusion tensor leads to imprecise mean diffusivity values, over-estimates of diffusion anisotropy, and poor assessment of the direction of principal diffusivity (9–12).

In this paper, previous work on the optimization of schemes to measure diffusion in isotropic media is reviewed and then developed to derive optimal schemes for measuring the diffusion tensor and its scalar invariants.

[1]Division of Medical Physics, University of Leicester, Leicester Royal Infirmary, Leicester LE1 5WW, United Kingdom.

[2]Departments of Neuroimaging, Maudsley and Kings College Hospitals, Denmark Hill, London SE5 8AZ, United Kingdom.

[3]Institute of Psychiatry, De Crespigny Park, London SE5 8AF, United Kingdom.

Grant sponsor: Wellcome Trust; Grant number: 043235/Z/94/Z.

*Correspondence to: Mark A. Horsfield, Division of Medical Physics, Leicester Royal Infirmary, Leicester LE1 5WW, UK.

Received 3 February 1999; revised 29 April 1999; accepted 20 May 1999.

THEORY

Diffusion in Anisotropic Systems

Diffusion in anisotropic systems can only be fully characterized by the symmetric 3 × 3 diffusion tensor matrix **D**:

$$\mathbf{D} = \begin{bmatrix} D_{xx} & D_{xy} & D_{xz} \\ D_{xy} & D_{yy} & D_{yz} \\ D_{xz} & D_{yz} & D_{zz} \end{bmatrix}, \quad [1]$$

where D_{xx}, D_{yy}, and D_{zz} relate the diffusional fluxes to the concentrations gradients in the *x*, *y*, and *z* directions and the off-diagonal terms reflect the correlation between diffusional fluxes and concentration gradients in orthogonal directions.

In a diffusion-weighted spin-echo MR experiment, the signal intensity resulting from the application of diffusion-encoding gradients is

$$S = S_0 e^{-\mathrm{TE}/T_2} e^{-(b_{xx}D_{xx}+b_{yy}D_{yy}+b_{zz}D_{zz}+2b_{xy}D_{xy}+2b_{xz}D_{xz}+2b_{yz}D_{yz})}, \quad [2]$$

where S_0 is the unweighted signal intensity, TE is the echo time, T_2 is the transverse relaxation time, and the 3 × 3 **b**-matrix is defined by:

$$\mathbf{b} = \gamma^2 \int_0^{\mathrm{TE}} \mathbf{F}(t')^T \mathbf{F}(t')\, dt'. \quad [3]$$

γ is the gyromagnetic ratio constant and **F** is a vector of the integral of the gradient amplitudes in the *x*, *y*, and *z* directions, with a negation of the integral occurring at the 180° refocusing pulse, for example:

$$F_x(t') = \int_0^{t'} G_x(t)\, dt \qquad 0 < t' \leq \mathrm{TE}/2 \quad [4a]$$

$$F_x(t') = \int_{\mathrm{TE}/2}^{t'} G_x(t)\, dt - F_x(\mathrm{TE}/2) \qquad \mathrm{TE}/2 < t' \leq \mathrm{TE}, \quad [4b]$$

where $G_x(t)$ is the time-dependent gradient in the *x* direction. The superscript *T* indicates the transpose of a vector.

In an experiment using rectangular diffusion-encoding gradient pulses of duration δ, and amplitude G, separated in time by Δ and applied, for example, along the *x* direction, Eq. [3] yields the Stejskal-Tanner expression for the *b*-factor in the *x* direction (13):

$$b_{xx} = \gamma^2 G^2 \delta^2 \left(\Delta - \frac{\delta}{3}\right). \quad [5]$$

Optimal Measurement of Isotropic Systems

The optimal measurement of isotropic diffusion coefficients has been addressed previously (1–8). In isotropic systems, the **D** matrix reduces to a single scalar, so that the attenuation equation can be written:

$$S = S_0 e^{-\mathrm{TE}/T_2} e^{-bD}, \quad [6]$$

where now b is the scalar b-factor defined by Eq. [3] and D is the apparent diffusion coefficient (ADC). Variation of the b-factor, while maintaining a constant echo time allows the diffusion coefficient to be estimated. If the diffusion coefficient is estimated from just two measurements, then the minimum error is achieved when the first measurement is made with minimum weighting, b_1, and the second with a weighting, b_2, such that $(b_2 - b_1)\ D \approx 1.11$ (4). If time permits more measurements to be made, then it has been shown (4,14) that just two b-factors should be used, with multiple measurements being made at each b-factor. In the limit of a very large number of measurements, the number of measurements at the high b-factor should be 3.6 times the number at the low b-factor, and the optimal difference in the b-factors is $1.28/D$.

Optimal Measurement of Anisotropic Systems

Estimation of the Trace of the Diffusion Tensor

Diffusion imaging in anisotropic systems, with diffusion-encoding gradients applied along just one axis results in rotationally variant image contrast. However, rotationally invariant image contrast can be achieved by computing all the components of the diffusion tensor matrix (15), and displaying scalar rotationally invariant properties of the tensor, such as the trace, denoted here as $Tr(\mathbf{D})$. It is possible to determine the tensor trace without first estimating the full tensor, by simply measuring the diffusivity in three orthogonal directions and adding these three diffusivities:

$$Tr(\mathbf{D}) = D_{xx} + D_{yy} + D_{zz}. \quad [7]$$

The minimum number of signal amplitude measurements required to estimate the trace in this way is four: one measurement without diffusion weighting, and one in each of three orthogonal directions. It is, of course, possible to give weight to a single image that is independent of tissue anisotropy (so-called ''trace weighting''); optimization of these schemes is addressed later in this section. If just four measurements are made, then minimizing the variance of the trace is equivalent to minimizing the variance of the individual diagonal elements of the tensor matrix. Thus, each individual measurement of D_{xx}, D_{yy}, and D_{zz} can be optimized in the same way as before with the optimal diffusion weightings along the x, y, and z axes, $(b_2 - b_1)_{xx}$, $(b_2 - b_1)_{yy}$, and $(b_2 - b_1)_{zz}$, respectively being equal to $1.11 \times 3 / Tr(\mathbf{D})$.

If a more precise assessment of $Tr(\mathbf{D})$ is needed, then more measurements should be made. To optimize the measurement, it is assumed that, in common with the findings of Bito et al. (4) and Eis et al. (14) for optimal schemes for estimation of isotropic diffusion coefficients, just 2 b-factors are used—a zero (or very low) b-factor and a high b-factor. If a total number of measurements, N, of signal attenuation are made, with the number of measurements with the low b-factor being N_L, and the number with each high b-factor being N_H, then $N = N_H + N_L$. Note that, without loss of generality, the lower b-factor (b_1) can be set to zero and thus the difference in b-factors ($b_2 - b_1$) is equal to the amplitude of the higher b-factor (b_2).

D_{xx} is estimated from the following expression:

$$D_{xx}(\mathrm{est}) = -\frac{\ln (S_{xx}/S_0)}{b_{xx}}, \quad [8]$$

where b_{xx} is the b-factor when the diffusion weighting gradients are applied in the x direction, S_{xx} is the resulting signal intensity, and S_0 is the signal intensity without the diffusion encoding gradients applied. The error in the estimate of D_{xx} can be derived by considering the propagation of errors (16) to give

$$\sigma_{D_{xx}(est)} = e^{\mathrm{TE}/T_2} \frac{\sigma_{S_0}}{S_0} \frac{1}{b_{xx}} \sqrt{\frac{1}{N_L} + 3\left(\frac{e^{2b_{xx}D_{xx}}}{N - N_L}\right)}, \quad [9]$$

where σ_{S_0} is the error in the measurement of S_0. Minimization of Eq. [9] with respect to both b_{xx} and N_L gives optimum values of $b_{xx} = 1.18/D_{xx}$, and $N_L = 0.151N$. Thus, the optimal ratio of the number of measurements with each of the high b-factors to the number of measurements at the low b-factor is 1.87:1 when N is large. The b-factors in the y and z directions would similarly be $1.18 / D_{yy}$ and $1.18 / D_{zz}$ and, with no a priori knowledge about the anisotropy of the tensor, all three optimal b-factors would be $1.18 \times 3/Tr(\mathbf{D})$.

The above scheme is optimal for diffusion tensors that deviate only slightly from isotropy. However, for highly anisotropic tensors it can be seen that in the direction of least restriction, signal attenuation will be very high, while in the direction of greatest restriction there will be much less signal attenuation. Thus, although the tensor trace may be fairly uniform over, for example, a subject's cerebrum (9), regions of anisotropy will lead to a suboptimal set of individual attenuation measurements. Because we assume no a priori knowledge of the degree of tissue anisotropy, or how the orientation of the principal axes vary from point to point within the image, measurements in individual directions cannot be optimized. Any directional bias inherent in making measurements in a fixed set of orthogonal directions can be reduced as far as possible, however, by spreading out the measurements in 3-dimensional gradient-vector space. The ratio of the total number of measurements with high diffusion weighting to the number with low diffusion weighting should still be maintained at 5.61:1 (i.e., 3×1.87:1), but now only 1 measurement should be made in each direction.

The total number of measurements (N_{TOTAL}) for trace estimation via this method is:

$$N_{TOTAL} = N_L + 3N_{sets}, \quad [10]$$

where N_L is the number of measurements made at the low (or zero) b-value and N_{sets} is the number of sets of three orthogonal gradient vectors. If more than one orthogonal

set is to be employed, the minimum value of N_{TOTAL} in the series given by Eq. [10] is 7 (i.e., $N_L = 1$, $N_{sets} = 2$). This is also the minimum number of measurements required to estimate all elements of the diffusion tensor matrix. However, if the only tensor property of interest is the trace, then it can be obtained with much less computation than that required for estimating the tensor.

Gradient Vector Orientations for Estimating the Trace

Without prior knowledge about the orientation of the tensor, the criterion adopted for optimizing the relative orientations of sets of orthogonal gradient vectors is that they should be uniformly distributed in 3-dimensional space. Conturo et al. (17) observed that the optimal arrangement of four vectors (i.e., tetrahedral) also occurs in nature to uniformly balance electrostatic repulsion in chemical sp^3 hybrid orbitals. The algorithm derived in the current study to find the optimal arrangement of N gradient vectors follows on from this observation, again involving an analogy with electrostatic repulsion.

Consider a model in which a line parallel to each gradient vector passes through the center of a sphere, and a unit electrical charge is placed at both of the points where the line intersects the surface of the sphere. Each gradient vector is represented by a pair of points in this way because a diffusion attenuation measurement with the gradient in a positive direction could equally well have been performed with the gradient in the opposite direction, since the diffusion tensor is symmetric in the absence of charged moieties. The repulsive force between a pair of charges is, according to Coulomb's law, inversely proportional to the square of the distance between the charges. The algorithm used to arrange the gradient vectors uniformly in 3-dimensional space therefore adjusts the orientations of the sets of orthogonal gradient vectors until the sum of the repulsive forces between every possible pair of charges is minimized. This is accomplished using the downhill simplex method of Nelder and Mead (18). Table 1 suggests some suitable gradient vectors when using 1, 2, and 3 sets of orthogonal gradient vectors.

Estimation of the Diffusion Tensor

Optimization of the tensor measurement again involves two parts: the choice of the set of gradient vector directions and the optimization of the set of *b*-factors and numbers of measurements made with each *b*-factor.

The algorithm used for selecting gradient orientations for estimation of the diffusion tensor uses the same analogy of electrostatic repulsion used in the previous section. However, each gradient vector can now be considered independently because there is no need to maintain orthogonality between sets of gradient vectors. The algorithm results in some familiar orientations for small numbers of gradients: orthogonal for three gradients and tetrahedral (17) for four. Table 2 shows some sets of gradient vector orientations for larger numbers of vectors useful when estimating the diffusion tensor. Note that the tetrahedral set of four gradient vectors has been used by others (17,19) for estimation of the tensor by assuming that the tensor ellipsoid possesses axial symmetry.

From Eq. [2], it is seen that estimation of the diffusion tensor matrix requires a minimum of seven measurements of signal intensity to be made (since the non-diffusion-weighted intensity must also be estimated) with gradients applied in at least six noncollinear directions. Because this seven-measurement case is the simplest to understand, attention will be given to optimizing the *b*-factors for this case and the result later generalized to a greater number of gradient directions. Even in this simplest of cases, the analysis generated expressions that were too large to be manipulated by hand; therefore, the symbolic computation package Maple (University of Waterloo, Ontario, Canada) was used.

First, for the set of six gradient orientations given in Table 2, the six unique components of the diffusion tensor were found in terms of the seven attenuation values by solution of seven simultaneous equations resulting from the gradient vectors being substituted into Eq. [2]. Next, the variances of each of the unique elements of the diffusion tensor were written from consideration of the propagation of errors (16). For example, the variance in the estimate of D_{xx} is given by Eq. [11]:

$$\sigma^2_{D_{xx}(est)} = \left(\frac{\partial D_{xx}(\text{est})}{\partial S_0}\right)^2 \frac{\sigma_2}{N_L} + \sum_{i=1}^{6} \left(\frac{\partial D_{xx}(\text{est})}{\partial S_i}\right)^2 \frac{\sigma^2}{(N - N_L/6)} \quad [11]$$

where N_L is again the number of measurements with low diffusion weighting, S_0 is the signal intensity measured without diffusion weighting, and S_1 to S_6 are the intensities

Table 1
Recommended Gradient Unit Vectors for Estimating the Trace of the Diffusion Tensor Using 1, 2, and 3 Sets of Three Orthogonal Gradients*

Number of gradient vectors		*x* *y* *z*		Components of gradient vector orientation					
	1.000	0.000	0.000						
3	0.000	1.000	0.000	—	—	—	—	—	—
	0.000	0.000	1.000						
	1.000	0.000	0.000	−0.666	0.334	−0.667			
6	0.000	1.000	0.000	−0.333	0.667	0.667	—	—	—
	0.000	0.000	1.000	0.667	0.667	−0.333			
	1.000	0.000	0.000	−0.708	−0.503	−0.496	0.517	0.490	0.702
9	0.000	1.000	0.000	−0.706	0.508	0.493	0.475	0.518	−0.711
	0.000	0.000	1.000	0.004	0.699	−0.715	−0.713	0.701	0.035

*When more than one set of orthogonal gradients is employed, the sets are arranged so as to sample 3-dimensional space as uniformly as possible. The orientations were derived using an algorithm based on analogy with electrostatic repulsion.

Table 2
Recommended Arrangements of Unit Gradient Vectors for Estimating the Diffusion Tensor Matrix*

Number of gradient vectors			x y z	Components of gradient vector orientation						
	1.000	0.447	0.447	0.447	0.447	−0.447				
6	0.000	0.895	0.277	−0.724	−0.724	−0.277	—	—	—	—
	0.000	0.000	0.850	−0.525	0.525	0.850				
	1.000	0.333	−0.333	0.577	0.333	−0.577	0.577			
7	0.000	0.943	0.472	−0.817	−0.472	−0.407	0.407	—	—	—
	0.000	0.000	0.817	0.000	0.817	0.707	0.707			
	1.000	0.488	−0.200	0.678	0.119	−0.686	0.631	−0.229		
8	0.000	0.873	0.266	−0.700	−0.599	−0.324	0.265	0.876	—	—
	0.000	0.000	0.942	0.224	0.792	0.651	0.729	0.425		
	1.000	0.251	−0.078	0.604	0.000	−0.723	0.671	−0.488	0.548	
9	0.000	0.968	0.116	−0.786	−0.691	−0.366	−0.178	0.628	0.606	—
	0.000	0.000	0.990	0.133	0.723	0.586	0.720	0.606	0.577	
	1.000	0.678	−0.556	0.672	0.012	−0.680	−0.045	−0.024	0.458	0.658
10	0.000	0.735	0.504	−0.733	−0.801	−0.310	−0.011	0.966	0.521	−0.250
	0.000	0.000	0.661	0.106	0.598	0.664	0.999	0.257	0.721	0.710

*As in Table 1, the relative orientations of the gradient vectors were derived using an analogy with electrostatic repulsion.

when the six diffusion weighting gradient vectors shown in Table 2 are applied.

Precise estimation of the tensor requires that the variance of each of the elements of the tensor matrix is minimized. Equal importance is assigned to each of the unique elements and therefore the summed variance is differentiated with respect to the higher *b*-factor (b_2) in each of the gradient vector directions, and with respect to N_L. *Thus,*

$$\frac{\partial}{\partial b_2}(\sigma^2_{D_{xx}(est)} + \sigma^2_{D_{yy}(est)} + \sigma^2_{D_{zz}(est)} + \sigma^2_{D_{xy}(est)} + \sigma^2_{D_{xz}(est)} + \sigma^2_{D_{yz}(est)}) = 0, \quad [12a]$$

and

$$\frac{\partial}{\partial N_L}(\sigma^2_{D_{xx}(est)} + \sigma^2_{D_{yy}(est)} + \sigma^2_{D_{zz}(est)} + \sigma^2_{D_{xy}(est)} + \sigma^2_{D_{xz}(est)} + \sigma^2_{D_{yz}(est)}) = 0. \quad [12b]$$

Numerical solution of these two simultaneous equations, when the tensor was assumed to be isotropic yielded: $b_2(\text{opt}) = 1.09/D_{xx}$ and $N_L = 0.081N$ for large N. Thus, the ratio of the number of measurements with each of the high *b*-factors to the low *b*-factor is 1.89:1 when N is large. If only one measurement is made in each of the gradient vector directions, together with an unweighted measurement (i.e., N is fixed at 7, and N_L is fixed at 1) then consideration of Eq. [12a] alone gives $b_2(\text{opt}) = 1.05/D_{xx}$.

It should be reiterated here that the results in this section were obtained assuming that the lower *b*-factor (b_1) was zero. If b_1 is not zero, then the optimal difference in *b*-factors, $(b_2 - b_1)_{\text{opt}} = 1.09/D_{xx}$ when N is large and $(b_2 - b_1)_{\text{opt}} = 1.05/D_{xx}$ when $N = 7$. Of course, b_1 (and therefore b_2) should be chosen to be as low as possible subject to this constraint, so as to maximize the available signal-to-noise ratio.

Again, we suggest that if more measurements than the minimum of seven are to be made, then the bias introduced by measuring signal attenuation along a limited number of gradient directions is reduced by using more gradient vector directions chosen from Table 2. The ratio of the total number of measurements with high diffusion weighting to the number at the low diffusion weighting should be maintained at approximately 11.3:1, but with only 1 measurement for each diffusion-encoding gradient vector direction.

Isotropic Diffusion Weighting

Pulse sequences have been proposed in which the signal is attenuated by the trace of the tensor matrix (20, 21). These sequences involve bipolar gradient waveforms applied simultaneously in the *x*, *y*, and *z* directions such that $b_{xx} = b_{yy} = b_{zz} \neq 0$ and $b_{xy} = b_{xz} = b_{yz} = 0$. The resulting signal intensity is:

$$S = S_0 e^{-(b_{xx}D_{xx} + b_{yy}D_{yy} + b_{zz}D_{zz})} = S_0 e^{-b_{xx}Tr(\mathbf{D})}. \quad [13]$$

Thus, the trace can be estimated from the isotropically weighted signal intensity and the unweighted signal intensity. It is straightforward to show that for just a pair of measurements the optimal value for b_{xx} is $1.19/Tr(\mathbf{D})$, and for multiple measurements it is $1.28/Tr(\mathbf{D})$ with the ratio of the number of measurements with trace weighting to unweighted being 3.6:1.

Effect of T_2-Weighting on Optimal ADC and Trace Estimation

The above analysis assumes that any desired *b*-factor can be achieved without penalty. However, because of the finite magnetic field gradient strengths that are achievable, increasing the *b*-factor may necessitate increasing the echo time, allowing more time for transverse relaxation, and hence, diminished signal-to-noise ratio in both the unweighted and the diffusion-weighted signals. The optimal

pulse sequence, for a given *b*-factor, will therefore minimize the echo time and is subject to the following constraints:

The diffusion encoding gradients are applied for the maximum possible duration within the echo time.

The amplitude of the diffusion-encoding gradients for the higher *b*-factor is the maximum achievable, G_{max}.

Figure 1 shows the relevant timing parameters for optimizing an echo planar imaging (EPI) pulse sequence subject to the above constraints. For full sampling of *k*-space, the maximum duration of the second diffusion encoding gradient pulse is dictated by the time required for the imaging gradients during signal acquisition. The time required for these gradients is denoted t_A so that the maximum possible duration, δ, of each diffusion-encoding gradient pulse is

$$\delta = \left(\frac{TE}{2} - t_A\right). \quad [14]$$

The maximum separation of the gradients, Δ, also depends on the echo time and a time for imaging gradients (denoted t_B), which is also dependent on the pulse sequence design:

$$\Delta = \left(\frac{TE}{2} - t_B\right). \quad [15]$$

For the sequence used in this work (see Fig. 1), $t_A = SSRC + tEPI$ and $t_B = SSRC - tRF_1$ such that $\delta = TE/2 - SSRC + tEPI$ and $\Delta = TE/2 + SSRC - tRF_1$.

When these expressions for δ and Δ are substituted into the Stejskal-Tanner expression (Eq. [5]), the expression for the maximum achievable *b*-factor b_{max} for a given echo time, becomes a cubic in TE. The echo time can thus be expressed in terms of b_{max} by solving this cubic equation (18) to give

$$TE = \left(\kappa + \frac{\beta}{\kappa} - \epsilon\right), \quad [16]$$

where

$$\kappa = [|\alpha| + \sqrt{\alpha^2 - \beta^3}]^{1/3}, \quad [17a]$$

$$\alpha = t_A^2(t_A + 3t_B) + t_B^2(t_B + 3t_A) - 6b_{max}/\gamma^2 G_{max}^2, \quad [17b]$$

$$\beta = (t_A + t_B)^2, \quad [17c]$$

and

$$\epsilon = (t_A - t_B). \quad [17d]$$

If it is again assumed that a total of N measurements are made, with N_H measurements at a high *b*-factor (b_{max}) and $(N - N_H)$ at a low *b*-factor ($b = 0$), then by substituting Eq. [16] into Eqs. [12a] and [12b] and using the error propagation equation (16), an expression for the error in the estimate of the diffusion coefficient is obtained:

$$\sigma_D = \sigma \sqrt{\exp\left(\frac{2(\kappa + \frac{\beta}{\kappa} - \epsilon)}{T_2}\right)\left(\frac{N_H + (N - N_H).\exp(2b_{max}D)}{S_0^2 b_{max}^2 . N_H . (N - N_H)}\right)}. \quad [18]$$

Similarly, the error in the estimate of the trace, $\sigma_{Tr(\mathbf{D})}$, when N_H measurements are made in each of three orthogonal

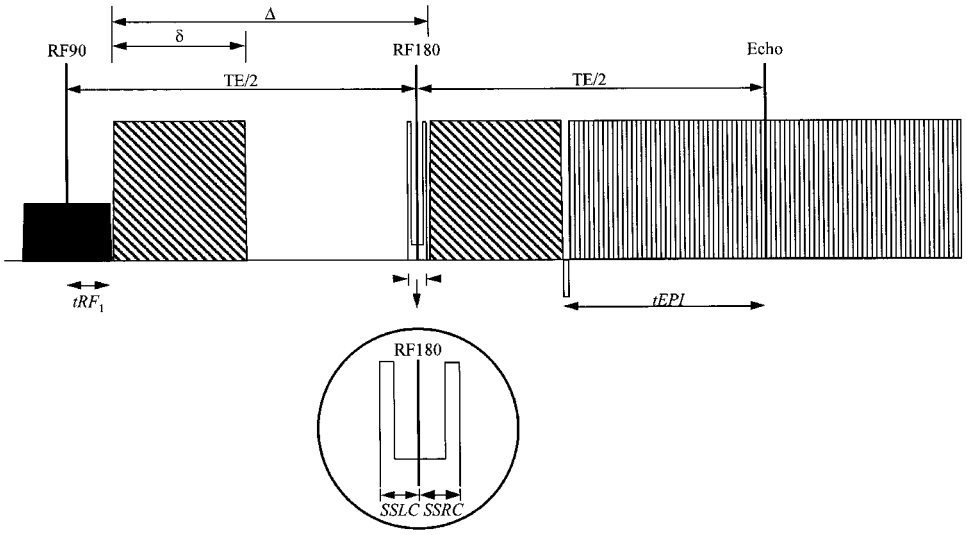

FIG. 1. Schematic showing the timing parameters that need to be considered when optimizing the diffusion-weighted spin-echo EPI pulse sequence used in this study. RF90 and RF180 indicate the positions of the 90° and 180° RF pulses. The echo time is TE. tRF_1 is the time from the center of the excitation pulse to the end of the gradient ramp down. *tEPI* is the required for the echo-planar dephase and readout gradients to the center of the spin-echo. The sum of the duration of the left crusher gradient (slice-select axis) and half the duration of the slice-select gradient for the refocusing pulse is *SSLC* and the sum of the duration of the right crusher gradient (slice-select axis) and half the slice-select gradient is *SSRC*. The duration of the diffusion encoding gradients is δ and their separation is Δ.

directions, is given by

$$\sigma_{Tr(\mathbf{D})} = \sigma \sqrt{\exp\left(\frac{2(\kappa + \frac{\beta}{\kappa} - \epsilon)}{T_2}\right)\left(\frac{N_H + (N - 3N_H).\exp\left(2b_{max}\frac{Tr(\mathbf{D})}{3}\right)}{S_0^2 b_{\max}^2 . N_H . (N - 3N_H)}\right)}. \quad [19]$$

It should be noted that similar expressions can be obtained for the variances in estimates of the ADC or trace in constant-gradient experiments by setting the time for the imaging gradients to zero, i.e., $t_A = t_B = 0$.

The optimal parameters for ADC and trace estimation are obtained by minimizing Eq. [18] and Eq. [19] with respect to N_H and $b_{\max}$. Because an analytical solution has not been found for the optimal values of $b_{\max}$ and N_H, the minima were found numerically using the downhill simplex method (18). Figure 2 shows the optimal parameters for estimating the ADC and the trace as a function of T_2, for our scanner, where $G_{\max} = 22$ mT m^{-1}. The optimal ratio of measurements shown for measuring the trace is the ratio of number of measurements made at the higher *b*-factor to the low *b*-factor in each direction. Note that the long T_2 asymptotes of the ratio of the number of measurements at each *b*-factor and the separation of *b*-factors are the same as those obtained earlier, but that in the range of T_2 typical of brain tissue, there is a strong T_2 dependence.

Effect of T_2-Weighting on Optimal Parameters for Estimating the Tensor

The effects of accounting for transverse relaxation in the optimization procedure are now considered in more detail and an attempt is made to extend this to the optimization of schemes for estimating the diffusion tensor.

Figure 3a shows the T_2 dependence of the optimal *b*-factor for estimation of the ADC and trace as a fraction of the long T_2 asymptotic values shown in Fig. 2. Note that the lines for optimal ADC measurement and optimal trace measurement follow each other closely over the range 20 to

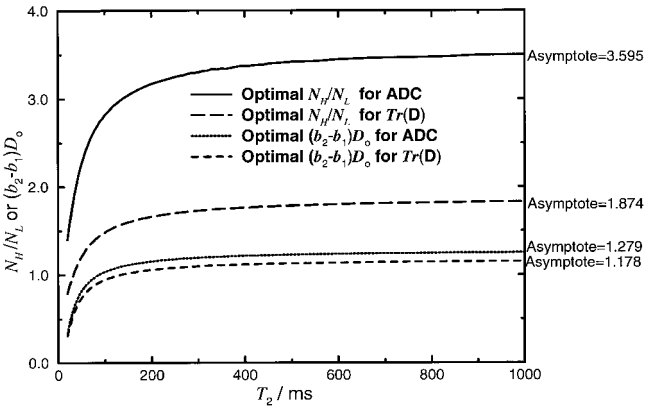

FIG. 2. Optimal values of $(b_2 - b_1)D_0$ and ratio of measurements made at higher *b*-factor to lower *b*-factor (N_H/N_L) as a function of T_2. The asymptotic values (i.e., as $T_2 \rightarrow \infty$) are given on the right-hand side of the vertical axis.

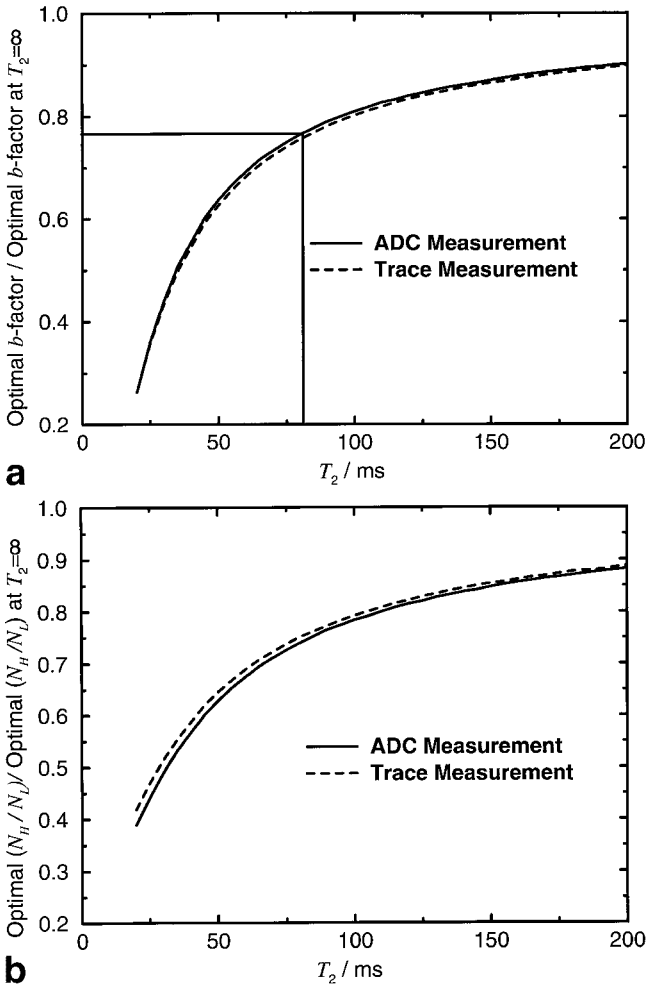

FIG. 3. **a:** Variation in the optimal value of $(b_2 - b_1)D_0$ (as a fraction of value at $T_2 = \infty$) for estimation of ADC and trace as a function of T_2. **b:** Variation in the optimal ratio (N_H/N_L) of measurements made at higher *b*-factor to number made at lower *b*-factor (as a fraction of value at $T_2 = \infty$) for estimation of ADC and trace, as a function of T_2.

200 ms. It is assumed that the optimal diffusion weighting for estimation of the tensor matrix also follows this pattern. Based on this assumption, it is seen that at T_2 values typical of healthy white matter [i.e., 80 ms (22)], the optimal *b*-factor for estimating the tensor is approximately 77% of the asymptotic value obtained from the simultaneous solution of Eqs. [12a] and [12b]. Thus, the optimal diffusion weighting for healthy white matter using the pulse sequence in Fig. 1 is estimated to be $(b_2 - b_1) = 0.85/D \approx 1035$ s mm^{-2}.

Figure 3b shows the T_2 dependence of the optimal ratio of the number of measurements made at the higher *b*-factor to the number made at the lower *b*-factor (N_H/N_L). In the same way that the optimal diffusion weighting for estimation of the tensor was found from Fig. 3a, the optimal value of N_H/N_L at $T_2 = 80$ ms was also found to be approximately 77% of the long T_2 asymptote. Thus, for estimation of the tensor in tissue in healthy white matter, using the pulse sequence shown in Fig. 1, the optimal ratio of the number of measurements made at the higher *b*-factor to the number made at the lower *b*-factor is taken to be approximately 77% of the long T_2 asymptote value and is therefore 8.7:1.

MATERIALS AND METHODS

MR Imaging System

Diffusion-weighted MR data were acquired from both a water phantom doped with Cu_2SO_4 and the cranium of a healthy volunteer (26 years), using a 1.5-T GE Signa Echospeed system (General Electric, Milwaukee, WI) with actively shielded magnetic field gradients (maximum amplitude, 22 mT m^{-1}). A quadrature birdcage head coil was used for both RF transmission and NMR signal reception, for both phantom and volunteer studies. In the volunteer studies, the subject's head was secured in the head coil by means of foam padding and a restraining strap stretched across the forehead.

Pulse Sequences

The pulse sequence used for all image acquisitions was a pulsed gradient spin-echo sequence with echo planar read-out depicted schematically in Fig. 1. The field of view was 240 mm × 240 mm with an acquisition matrix of 96 × 96 and a reconstruction matrix of 128 × 128 pixels. The slice thickness was 5 mm with an interslice gap of 2.5 mm. For phantom studies, the repetition time (TR) was 3 s, and for volunteer studies the acquisition was peripherally gated to the cardiac cycle with an effective TR of 4 R-R intervals (trigger delay = 200 ms). The echo time, diffusion-encoding gradient waveforms (amplitudes, durations, vector directions) and number of measurements made at each diffusion weighting were varied according to the medium being imaged (phantom or human brain) and the sequence under evaluation.

Conventional Scheme

Prior to the optimization procedures outlined above, the imaging scheme employed in our institution for estimation of the tensor (termed here the *conventional* scheme), involved measurement of signal attenuation along 7 noncollinear directions (*x*, *y*, *z*, *xy*, *xz*, *yz*, and *xyz*) with N_b *b*-factors (equally spaced in *b*) per direction [e.g. (23)]. The maximum *b*-factors for phantom and human studies were 582 s mm^{-2} and 1410 s mm^{-2}, respectively (i.e., approximately $3.3/Tr(\mathbf{D})$ in both cases). The echo times used were the minimum necessary to achieve these *b*-factors.

Optimized Schemes

The parameters for the optimal schemes (echo time, δ, Δ, ratio of measurements made at each *b*-factor, orientation of gradient vectors) were derived for each measurement based on the estimated mean diffusivity and T_2 of the medium being studied and total number of measurements, using the method outlined above. The T_2 of the phantom had previously been determined to be 62 ms and the T_2 of white matter was taken to be 80 ms (22).

Comparison of Pulse Sequences

To compare the results from two pulse sequences with different parameters, the total number of measurements made with each pulse sequence was kept the same, allowing comparison of results for equivalent scan times. In some cases this necessitated a large total number of measurements being made. For example, the total number of measurements made with the conventional scheme (in which the diffusion gradients are applied in only 7 noncollinear directions) was required to be a multiple of 7, while the ratio of measurements made at the high *b*-factor to the number made at the low *b*-factor with the optimized scheme had to approximate the theoretical optimal value. The details of the experiments designed subject to these constraints are given below.

Table 3 lists the experiments performed to compare the optimized and conventional pulse sequences for tensor estimation in a water phantom. Table 4 lists the experiments performed to compare the optimized and conventional pulse sequences for tensor estimation in brain parenchyma. Table 5 lists the experiments performed to investigate the effect of varying the ratio of the number of measurements made at the higher *b*-factor to the number made at the lower *b*-factor. All other parameters were maintained at the optimal value, and the total number of measurements made with each pulse sequence for this last set of measurements was 56.

Analysis

Data were analyzed on an independent workstation (Sun Sparcstation Ultra 140, Sun Microsystems, Mountain View, CA). The diffusion-weighted images were first corrected for the effects of eddy current-induced distortion using

Table 3
Details of Experiments to Compare the Optimized and Conventional Pulse Sequences for Estimation of the Diffusion Tensor in a Water Phantom*

Exp. no.	Scheme type	Scheme details	N_{TOTAL}	Max. *b*-factor	N_{high}/N_{low}	δ (ms)	TE (ms)	TR (ms)
1	Conventional Tensor Sequence	4 *b*-vals/direction 7 directions	28	582	N.A.	19.64	109.0	3000
2	Optimised Tensor Sequence	3 low *b*-vals 25 high *b*-vals	28	453	8.33	17.59	104.9	3000
3	Conventional Tensor Sequence	8 *b*-vals/direction 7 directions	56	582	N.A.	19.64	109.0	3000
4	Optimized Tensor Sequence	6 low *b*-vals 50 high *b*-vals	56	453	8.33	17.59	104.9	3000

*N_{TOTAL}, the total number of measurements of signal attenuation made with a particular pulse sequence; Max. *b*-factor, the maximum *b*-factor (in units of s mm^{-2}) applied in any direction; N_{high}/N_{low}, the ratio of the number of measurements made at the higher *b*-factor to the number made at the lower *b*-factor when just two *b*-factors are used.

Table 4
Details of Experiments Performed to Compare the Optimized and Conventional Pulse Sequences for Estimation of the Diffusion Tensor in a Healthy Volunteer*

Exp. no.	Scheme type	Scheme details	N_{TOTAL}	Max. *b*-factor	N_{high}/N_{low}	δ (ms)	TE (ms)	TR
5	Conventional Tensor sequence	11 *b*-vals/direction 7 directions	77	1410	N.A.	28.66	127.0	4 R-R
6	Optimised Tensor sequence	8 low *b*-vals 69 high *b*-vals	77	1048	8.63	25.68	121.1	4 R-R
7	Conventional Tensor sequence	4 *b*-vals/direction 7 directions	28	1410	N.A.	28.66	127.0	4 R-R
8	Optimised Tensor sequence	3 low *b*-vals 25 high *b*-vals	28	1048	8.33	25.68	121.1	4 R-R

*N_{TOTAL}, the total number of measurements of signal attenuation made with a particular pulse sequence; Max. *b*-factor, the maximum *b*-factor (in units of s/mm^{-2}) applied in any direction; N_{high}/N_{low}, the ratio of the number of measurements made at the higher *b*-factor to the number made at the lower *b*-factor when just two *b*-factors are used. The repetition time was equal to 4 R-R intervals.

in-house software. For each data set, a reference image was first constructed by calculating the mean intensity in each voxel from all the non-diffusion-weighted images. Next, for each diffusion-weighted image the downhill simplex method (18) was used to select the optimal magnification, shear and displacement of the diffusion-weighted images in order to give the best registration with the reference image. The *mutual information* (24) was used to assess the registration between the *reference* image and the corrected image. Correction of each distorted image took approximately 30 s and so, for example, it took approximately 50 min to correct a four-slice data set acquired using the sequence used in Experiment 2. Note that in correcting for uniform magnification, shear, and displacement of the images, it was implicitly assumed that any eddy current-induced gradient was constant throughout the slice during the EPI readout. A more sophisticated approach would be to correct for image distortions due to eddy currents with time dependence during the EPI readout (e.g. Ref. 25).

Following correction of image distortion, the diffusion tensor was calculated for each voxel using multivariate linear regression after logarithmic transformation of the signal intensities (16). The tensor matrix in each voxel was subsequently diagonalized to compute the eigen values, and images of the tensor trace and fractional anisotropy (26) were created. The *dispim* image display program (David Plummer, University College Hospital, London) was used to define regions of interest and analyze the data.

RESULTS

Conventional vs. Optimized Diffusion Tensor Pulse Sequences in Water Phantom

The results from Experiments 1 to 4 described in Table 3 are given in Table 6, which shows the mean and standard deviation in the estimates of the trace, and fractional anisotropy measured in the center of a water phantom.

Conventional vs. Optimized Diffusion Tensor Pulse Sequences in Human Brain

Figure 5 shows fractional anisotropy images at two slice positions obtained from the volunteer using 4 different sequences (Experiments 5–9 in Table 4). The gray scale is linearly scaled with anisotropy so that the most anisotropic tissue (white matter) appears brightest, while less anisotropic tissue appears less bright.

Optimization of N_{high}/N_{low} for Tensor Estimation

Figure 4a shows the standard deviation of the diffusivity measured in a region of interest placed in the center of the phantom as a function of the ratio of measurements made at the higher *b*-factor to the lower *b*-factor (Experiments 9–13 in Table 5). Figure 4b similarly shows the mean fractional anisotropy measured in the same region of interest.

Table 5
Details of Experiments Performed to Verify the Optimal Ratio of the Number of Measurements Made at the Higher *b*-Factor to the Number Made at the Lower *b*-Factor for Estimation of the Tensor in a Water Phantom*

Exp. no.	Scheme type	Scheme details	N_{TOTAL}	Max. *b*-factor	N_{high}/N_{low}	δ (ms)	TE (ms)	TR (ms)
9	Tensor sequence	11 low *b*-vals 45 high *b*-vals	56	453	4.09	17.59	104.9	3000
10	Tensor sequence	8 low *b*-vals 48 high *b*-vals	56	453	6.00	17.59	104.9	3000
11	Tensor sequence	6 low *b*-vals 50 high *b*-vals	56	453	8.33	17.59	104.9	3000
12	Tensor sequence	5 low *b*-vals 51 high *b*-vals	56	453	10.20	17.59	104.9	3000
13	Tensor sequence	4 low *b*-vals 52 high *b*-vals	56	453	13.00	17.59	104.9	3000

*N_{TOTAL}, the total number of measurements of signal attenuation made with a particular pulse sequence; Max. *b*-factor, the maximum *b*-factor (in units of s/mm^{-2}) applied in any direction; N_{high}/N_{low}, the ratio of the number of measurements made at the higher *b*-factor to the number made at the lower *b*-factor when just two *b*-factors are used.

Table 6
Trace and Fractional Anisotropy Measurement in a Water Phantom

Exp. no.	1	2	3	4
$Tr(\mathbf{D})$	6.02×10^{-3} mm^2 s^{-1}	5.95×10^{-3} mm^2 s^{-1}	6.02×10^{-3} mm^2 s^{-1}	5.99×10^{-3} mm^2 s^{-1}
$\sigma_{Tr(D)}$	0.11×10^{-3} mm^2 s^{-1}	0.07×10^{-3} mm^2 s^{-1}	0.08×10^{-3} mm^2 s^{-1}	0.05×10^{-3} mm^2 s^{-1}
FA	0.063	0.028	0.040	0.014
σ_{FA}	0.029	0.023	0.025	0.020

Results from the experiments listed in Table 3. $Tr(\mathbf{D})$ and $\sigma_{Tr(D)}$ are the mean and standard deviation in the estimates of the trace, respectively, and FA and σ_{FA} are the mean and standard deviation of the fractional anisotropy measured in the center of the water phantom.

DISCUSSION

The results from the water phantom clearly demonstrate the advantages of using the optimization strategy. The standard deviation in the estimate of the trace serves as a readily interpretable indicator of the precision of the diffusion tensor estimation. Measured diffusion anisotropy in an isotropic medium also acts as a sensitive indicator of precision, because any measured anisotropy must be attributable to errors in the estimation of the tensor.

The standard deviation in the trace estimate is reduced by more than 30% and the measured anisotropy in the water phantom is reduced by more than 55% when using the optimized schemes. However, there appears to be a systematic bias, with the estimate of the trace being lower when using the optimized pulse sequences. Issues of accuracy will be addressed later in this section. Note that for both the optimized and conventional pulse sequences, the error in the estimate of the trace with a total of 28 measurements is approximately $\sqrt{2}$ times greater than with 56 measurements, as would be expected from the theory.

Figure 4a and b, support the theory developed above that the optimal ratio of the number of measurements made at the higher *b*-factor to that at the lower *b*-factor for the water phantom is approximately 8.4. Figure 4a suggests that the optimal ratio of measurements derived when the effects of transverse relaxation are ignored (equal to 11.3) would result in a standard deviation in the estimate of the trace 15 to 20% greater than that when transverse relaxation is accounted for.

Figure 5 allows the advantage of using the optimized pulse sequences to be readily observed. There is a higher signal-to-noise ratio and improved contrast between white matter structures and the surrounding parenchyma when using the optimized pulse sequence for the same total number of measurements.

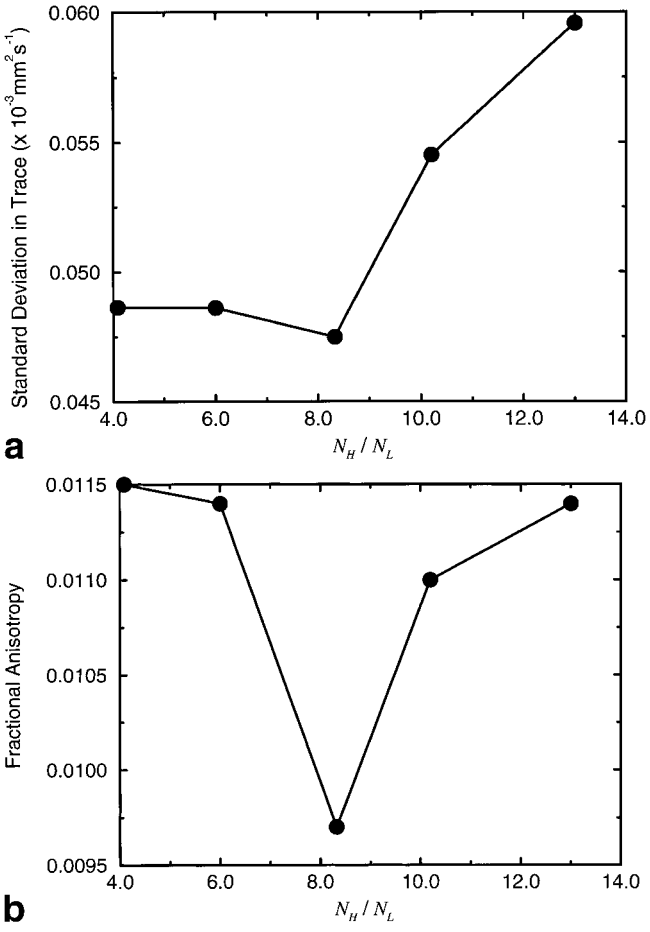

FIG. 4. Results from Experiments 9 to 13 showing (**a**) standard deviation in the estimate of mean diffusivity and (**b**) mean fractional anisotropy measured in a region of interest placed in the center of a large water phantom as a function of the number of measurements made with the high *b*-factor (N_H) to the number made with the low *b*-factor (N_L).

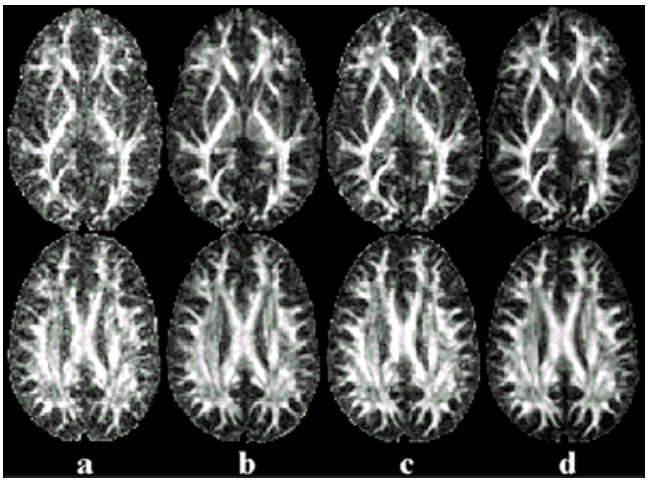

FIG. 5. Fractional anisotropy images at 2 slice positions acquired from a male volunteer (26 years) calculated from the diffusion tensor estimated using (**a**) conventional scheme with 4 *b*-factors applied in each of 7 non-collinear directions (*x*, *y*, *z*, *xy*, *xz*, *yz*, *xyz*); (**b**) optimized scheme with 3 measurements acquired with no diffusion weighting and 25 high *b*-factor measurements (gradient vectors uniformly distributed in space); (**c**) conventional scheme with 11 *b*-factors applied in each of 7 noncollinear directions; (**d**) optimized scheme with 8 measurements acquired with no diffusion weighting and 69 high *b*-factor measurements (gradient vectors uniformly distributed in space).

It is important to stress that the optimal parameters derived in this work were for a particular pulse sequence. However, the optimization procedure can be applied to any diffusion-weighted sequence if all timings are known.

This paper has described techniques to optimize the precision of quantitative estimates of diffusion in anisotropic systems. Improved precision results in higher signal-to-noise ratios in parametric diffusion images. Such improvements will, for example, lead to better definition of ischemic lesion volumes (5) through improved delineation of the ischemic lesion boundary. Optimization could alternatively be used to improve resolution with the same imaging time, enabling smaller structures to be seen.

We have derived optimal diffusion weightings and number of measurements made at each weighting for estimating the diffusion tensor trace and the complete diffusion tensor matrix. In order to reduce the scan time when estimating the diffusion tensor, some groups have modeled the diffusion tensor ellipsoid as having axial symmetry (17,19). Although we have not tackled the issue of estimating an axially symmetric tensor, we would expect our results to generalize to this case. The minimum number of measurements required to estimate an axially symmetric diffusion ellipsoid is 5 (one of which is unweighted). Thus, in common with the trace and full tensor matrix estimation, if transverse relaxation is ignored, we expected the optimal ratio of number of measurements at the higher *b*-factor to the number at the lower *b*-factor to be approximately 1.88:1 for a large total number of measurements, and the optimal diffusion weighting to be approximately $1.1 \times 3/Tr(\mathbf{D})$. Thus, approximately 7. 5 measurements should be made at the higher diffusion weighting for every measurement made at the lower diffusion weighting. As in the case of estimating the trace or complete tensor matrix, it would be expected that accounting for transverse relaxation in the manner described above would lead to a reduced optimal *b*-factor and ratio of the number of measurements.

While the optimization procedure described above minimizes the error in the estimate of diffusion due to random fluctuations in signal intensity, it is still possible that systematic errors persist in the measurement process. Minimization of such systematic errors may not be so critical for monitoring a disease state in which the change in diffusivity is of interest (as long as the systematic errors are constant and reproducible), but accuracy may be important in other applications of diffusion-weighted imaging. Potential sources of inaccuracy include the contributions of background gradients that are not included in the calculation of the *b*-matrix [see (27)] and the contributions from short time-constant eddy current-induced gradients that may not be uniform over the image slice during the EPI readout. Experiments 1 to 4 showed a systematic difference in the estimate of the trace (of the order of 1–2%) obtained with the optimized and conventional schemes. It is possible that the different gradient orientations used for sampling diffusion are responsible for this difference. The *cross-terms* between the background gradients and diffusion-encoding gradients and between eddy current-induced gradients and the diffusion-encoding gradients may change as a result of different gradient orientations. Also, if significant short time-constant eddy currents are generated, the distortion correction method used here would be inadequate. It is possible that different gradient orientations generate different eddy currents, which could again account for the differences in the mean diffusivities recorded in Experiments 1–4.

CONCLUSION

Optimal strategies for precise measurement of diffusion in anisotropic systems have been developed. Using these strategies should result in shorter scan times in diffusion imaging or improved quality of computed diffusion parametric images.

ACKNOWLEDGMENTS

Supported by the Wellcome Trust (grant number 043235/Z/94/Z), to whom the authors express their thanks.

REFERENCES

1. Ahn CB, Lee SY, Nalcioglu O, Cho ZH. An improved nuclear magnetic resonance diffusion coefficient imaging method using an optimized pulse sequence. Med Phys 1986;13:789–793.
2. Chien D, Buxton RB, Kwong KK, Brady T, Rosen BR. MR diffusion imaging of the brain. J Comput Assist Tomogr 1990;14:514–520.
3. Prasad PV, Nalcioglu O. A modified pulse sequence for in vivo diffusion imaging with reduced motion artefacts. Magn Reson Med 1991;28:116–131.
4. Bito Y, Hirata S, Yamamoto E. Optimal gradient factors for ADC measurements. In: Proceeding of the 3rd Annual Meeting of ISMRM, Nice, France, 1995. p 913.
5. Benfield A, Prasad PV, Edelman RR, Warach S. On the optimal *b*-value for measurement of lesion volumes in acute human stroke by diffusion-weighted imaging. In: Proceedings of the 4th Annual Meeting of ISMRM, New York, 1996. p 1344.
6. Benfield A, Griswald M, Jakob P, Edelman R, Warach S. Optimisation of diffusion weighted imaging: a theoretical approach to sequence programming. In: Proceedings of the 6th Annual Meeting of ISMRM, Vancouver, Canada, 1997. p 1747.
7. Xing D, Papadakis NG, Huang CLH, Lee VM, Carpenter TA, Hall LD. Optimized diffusion weighting for measurement of apparent diffusion coefficient (ADC) in human brain. Magn Reson Imaging 1977;15:771–784.
8. Pell GS, Thomas DL, Howseman AM, Houseman J, Gadian DG, Ordidge RJ. Optimisation of experimental parameters for diffusion-weighted single-shot trace measurements. In: Proceedings of the 5th Annual Meeting of ISMRM, Vancouver, Canada, 1997. p 1746.
9. Pierpaoli C, Basser PJ. Towards a quantitative assessment of diffusion anisotropy. Magn Reson Med 1996;36:893–906.
10. Bastin ME, Armitage PA, Marshall I. The effect of experimental noise on the calculation of diffusion anisotropy in diffusion tensor and diffusion-weighted imaging. In: Proceedings of the 6th Annual Meeting of ISMRM, Sydney, Australia, 1998. p 1220.
11. Skare S, Li TQ, Nordell B. Noise considerations of the anisotropy index in diffusion imaging. In: Proceedings of the 6th Annual Meeting of the ISMRM, Sydney, Australia, 1998. p 1231.
12. Basser PJ. Quantifying errors in fibre-tract direction and diffusion tensor field maps resulting from MR noise. In: Proceedings of the 5th Annual Meeting of ISMRM, Vancouver, Canada, 1997. p 1740.
13. Stejskal EO, Tanner JE. Spin diffusion measurements: spin-echoes in the presence of a time-dependent field gradient. J Chem Phys 1965;42: 288–292.
14. Eis M, Hoehn-Berlage M. Correction of gradient cross-talk and optimization of measurement parameters in diffusion MR imaging. J Magn Reson Ser B 1995;107:222–234.
15. Basser PJ, Mattiello J, Le Bihan D. MR diffusion tensor spectroscopy and imaging. Biophys J 1994;66:259–267.

16. Bevington PR, Robinson DK. Data reduction and error analysis for the physical sciences, 2nd edition. New York: McGraw-Hill; 1992.
17. Conturo TE, McKinstry RC, Akbudak E, Robinson BH. Encoding of anisotropic diffusion with tetrahedral gradients: a general mathematical diffusion formalism and experimental results. Magn Reson Med 1996;35:399–412.
18. Press WH, Teukolsky SA, Vetterling WT, Flannery BP. Numerical recipes in C: the art of scientific computing, 2nd edition. New York: Cambridge University Press; 1994. p 183.
19. Gulani V, Yang Y, Shimony JS, Chandra S, Lauterbur PC. Determination of orientation and diffusion anisotropy of parallel fibres using four diffusion measurements. In: Proceedings of the 2nd Annual Meeting of ISMRM, San Francisco, 1994. p 1040.
20. Wong EC, Cox RW, Song AW. Optimized isotropic diffusion weighting. Magn Reson Med 1995;34:139–143.
21. Mori S, van Zijl PCM. Diffusion weighting by the trace of the diffusion tensor within a single scan. Magn Reson Med 1995;33:41–52.
22. Whittall KP, MacKay AL, Graeb DA, Nugent RA, Li DKB, Paty DW. In vivo measurement of T_2 distributions and water content in normal human brain. Magn Reson Med 1997;27:34–43.
23. Jones DK, Williams SCR, Horsfield MA. Full representation of white-matter fibre direction on one map via diffusion tensor analysis. In: Proceedings of the 5th Annual Meeting of ISMRM, Vancouver, Canada, 1997. p 1743.
24. Studholme C, Hill DLG, Hawkes DJ. Automated three-dimensional registration of magnetic resonance and positron emission tomography brain images by multiresolution optimization of voxel similarity measures. Med Phys 1997;24:25–35.
25. Calamante F, Porter DA, Gadian DG, Connelly A. Correction for eddy current induced B_0 shifts in diffusion-weighted echo-planar imaging. Magn Reson Med 1995;41;95–102.
26. Basser PJ, Pierpaoli C. Microstructural and physiological features of tissue elucidated by quantitative-diffusion-tensor MRI. J Magn Reson Ser B 1996;111:209–219.
27. Conturo TE, McKinstry RC, Aronovitz JA, Neil JJ. Diffusion MRI: precision, accuracy and flow effects. NMR Biomed 1995;8:307–332.